GEOPHYSICAL RESEARCH LETTERS, VOL. 10, NO. 1, PAGES 51-54, JANUARY 1983

TIDAL-CURRENT CHANNELING IN THE SAN ANDREAS FAULT, CALIFORNIA

M.J.S. Johnston

U.S. Geological Survey, Menlo Park, California 94025

R.H. Ware

C.I.R.E.S., University of Colorado, Boulder, Colorado 80301

R. Mueller

U.S. Geological Survey, Menlo Park, California 94025

Abstract. Measurements of magnetic fields along the San Andreas fault indicate that inhomogeneous tidally generated current systems flow in and around the fault system. These currents limit measurements of short-term local fields of tectonomagnetic origin to about 0.3 nT but can be easily removed. Ocean-tidal induction into a complex fault zone with higher than average electrical conductivity appears to be a more likely explanation than either piezomagnetic effects due to solid-earth tides or ionospheric-tidal induction. The amplitudes of the induced diurnal harmonics decrease fairly linearly to the southeast along the fault. This result is consistent with expectations from a hotter and more conductive crust and upper mantle in southern California, as indicated by heat-flow data for this region.

Introduction

Ionospheric and magnetospheric disturbances contribute, both directly and indirectly, to surface measurements of magnetic fields and presently limit the precision to which local transient fields can be measured. Particularly important are the transient fields expected prior to and coincident with earthquakes [Stacey, 1964; Johnston, 1978]. While the problem of understanding the tensor nature of disturbance fields at particular sites is complex, several fairly simple techniques have been developed for isolating local fields by reducing the effects of unwanted large-scale fields. These techniques include the use of simple differences [Johnston et al., 1976], second differences [Ware, 1979], transfer functions [Beahn, 1976] and Weiner filters [Davis et al., 1981; Davis and Johnston, 1982].

In this paper we will investigate tidally generated magnetic noise in data obtained from the U.S. Geological Survey (USGS) magnetometer array near the San Andreas and other active faults in central and southern California. This source of noise presently limits the measurement precision of this array and implies details of fault structure and conductivity that have not been previously explored.

Paper number 2L1687.
0094-8276/83/002L-1687$3.00

Instruments and Data

The USGS has operated an array of continuously recording magnetometers along the San Andreas fault, since 1974. The array is designed to detect tectonomagnetic events within the fault system. Proton precession magnetometers, manufactured by Geometrics (model 816 or 826), and modified to 0.25-nT least-count uncertainty, are deployed in the array. The total field is measured simultaneously at all sites, every 10 minutes, and the data are then sent by telephone telemetry to the USGS Earthquake Studies Laboratory in Menlo Park, California. Figure 1 shows the locations of these 27 sites. Details of instrumentation, installation, telemetry, and operating procedures have been described by Mueller et al., [1981]. According to Mueller and Johnston [1981], the measurement precision with simple difference techniques throughout the array increases with distance as:

$$\sigma = a + bL$$

where σ is the standard deviation of hourly means of all the difference data, $a = 0.07 \pm 0.02$ nT, $b = 0.01 \pm 0.003$ nT/km, and L is the site separation in kilometers.

Here, we analyze two major types of data: total-field data from each of the 27 sites, and simple differences between 32 pairs of sites. In both cases, measurements taken at 10 minute intervals are averaged over 1 hour; the starting time is 0000 UT 1 January, 1980. Missing or unreasonable data are represented by an average value for the total field, and by interpolated values for the differences.

The most dominant feature of the total-field data is the roughly 30 nT Solar quiet (Sq) or diurnal variation, with occasional solar-driven magnetic storms, bays, and pulsations of similar or larger amplitude. Because of the global scale of these variations, simple differences from stations with up to a 10-km spacing allow more than a 97% reduction in their amplitude and subsequent isolation of smaller scale (< 1 nT) local fields [Johnston et al., 1976].

Analysis and Discussion

Clear indications of tidally generated fields are evident in the amplitude spectra of the total field time series, obtained using Fast

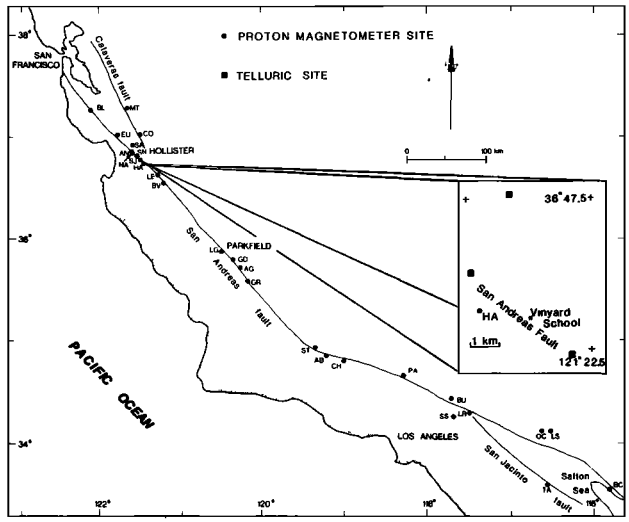

Fig. 1. USGS magnetometer (•) array and telluric (■) monitoring sites in central and southern California.

Fourier Transforms (FFT's) on three consecutive sets of 4096 hour averages of the data with nonharmonic noise removed, as shown in Figure 2. We attribute the solar harmonics in this spectrum principally to Sq variation and note the existence of the M_2 harmonic, with a period of 12.42 hours.

For all other sites in the array, we have computed the total-field solar and lunar harmonic amplitudes similarly (Table 1). In each computation, the fraction of missing data was determined, and the amplitudes were appropriately corrected. The M_2 amplitudes typically range from 0.2 to 1.0 nT.

There are three likely contributions to the M_2 peak 1) piezomagnetic effects due to solid-earth tides, 2) induction currents driven by ocean tides [Hewson-Browne, 1973; Malin, 1977], and 3) lunar semidiurnal currents in the ionosphere [Matsushita and Campbell, 1967].

Following Stacey and Bannerjee [1974] and using an optimistic value of 1 A/m for the total rock magnetization, the amplitude of the expected piezomagnetic tides is about 100 times smaller than that observed. The relative amplitude of ionospheric tides can be estimated from the fact that, since their source distance and frequency are similar, both Sq and ionospheric tides should be similarly attenuated in the difference-field data. This estimate is easily checked by comparing the amplitude spectra of the difference-field data with that of the total-field data. As illustrated in the amplitude spectrum of the SJ-SA differences (Figure 2), the amplitude of the M_2 peak is similar to that obtained in the total-field data from site SJ. If the source of this M_2 peak were in the ionosphere, we would expect the difference field M_2 peak to be not more than 10% of the total field M_2 (i.e., not more than 0.1 nT). This argument accounts for effects due to susceptibility, conductivity and magnetization contrasts between sites, because such contrasts are expected to influence ionospheric M_2 and S_2 equally. We conclude further that, because the maximum M_2 amplitudes of the difference-field data are comparable to the total field M_2 amplitudes, the source of these magnetic tides is inhomogeneous on a scale at least comparable to or less than the station separation.

Magnetic tides generated by the movement of conductive seawater through the Earth's magnetic field at tidal frequencies would explain these observations. The phase of these magnetic tides, although variable, corresponds roughly to the offshore tides at the Farallon Islands. However, some onshore current channeling is required to maintain the diverse M_2 amplitudes which are fairly independent of distance from the ocean and position along the fault. EU, the site closest to the ocean, has one of the smallest M_2 amplitudes, and BC, the station farthest from the ocean, one of the largest.

Little is known about the complex conductivity structure of the San Andreas fault system,

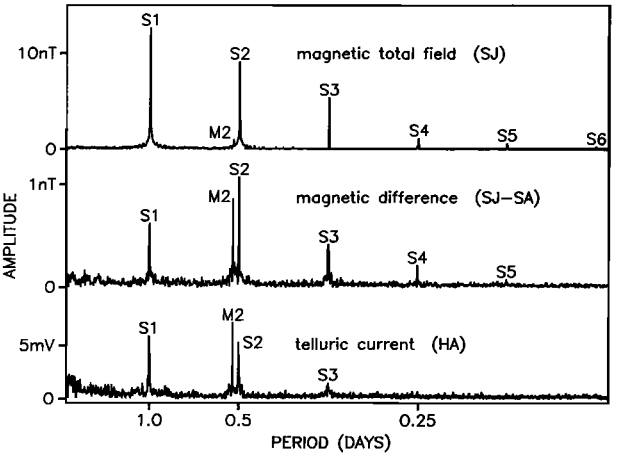

Fig. 2. Amplitude spectrum of total field data from SJ. The residual of SN, with S_1 through S_6 and M_2 removed, was subtracted from SJ to reduce non-harmonic noise. The central and lower plots show amplitude spectra of difference field (SJ-HA) and telluric potential field respectively.

Table 1. Total field harmonic amplitudes (nT), and phases (deg)

SITE	S_1	S_2	S_3	S_4	S_5	S_6	M_2
BL	14.4, -126.4	11.0, -52.6	5.6, 23.6	1.4, 121.7	.5, -54.3	.2, 55.2	.6, 152.7
MT	12.7, -126.4	9.1, -51.2	4.4, 25.9	1.1, 129.4	.5, -71.3	.2, 9.3	.5, 163.7
EU	14.1, -124.5	10.4, -50.3	5.2, 24.7	1.3, 122.6	.4, -67.5	1, 6.5	.3, -160.0
NA	12.9, -127.4	9.5, -49.1	4.8, 27.6	1.2, 131.0	.5, -65.1	.2, 26.7	.9, 146.1
AN	12.6, -127.0	9.2, -50.6	4.6, 20.9	1.2, 116.2	.5, -77.4	.1, 47.5	1.0, 129.4
CO	13.7, -126.2	10.0, -50.9	4.9, 25.5	1.1, 124.6	.5, -62.4	.2, 31.3	.3, 166.9
SA	13.8, -124.3	9.7, -48.7	4.9, 26.9	1.2, 125.4	.4, -65.1	1, 54.8	.4, -78.5
SN	14.5, -127.2	10.6, -52.2	5.1, 22.0	1.2, 121.1	.5, -70.7	.1, -2.0	.6, 148.4
SJ	14.7, -127.0	10.9, -51.9	5.4, 23.6	1.3, 123.1	.4, -60.4	.1, 49.7	.8, 149.7
HA	13.8, -128.3	10.0, -53.0	4.7, 23.1	1.1, 131.5	.7, -64.2	.3, 8.4	.8, 156.3
LE	14.0, -128.5	10.3, -52.8	4.9, 23.9	1.1, 132.6	.8, -57.4	.3, 8.7	.7, 163.6
BV	14.3, -128.0	10.4, -51.0	5.1, 25.6	1.2, 125.0	.5, -66.1	.2, 21.4	.7, 156.4
LG	13.1, -128.3	9.3, -46.5	4.4, 32.1	1.1, 134.5	.5, -43.8	2, 32.0	.2, -125.7
GD	13.0, -126.5	9.3, -47.2	4.4, 32.2	1.0, 138.9	.6, -47.0	.2, 39.3	.2, 166.3
AG	13.6, -128.9	9.4, -48.4	4.5, 30.6	1.1, 131.1	.4, -47.3	.1, 53.7	.3, 176.1
GR	13.8, -127.9	9.7, -48.2	4.7, 29.6	1.1, 131.5	.5, -40.4	.2, 54.9	.3, -134.6
ST	13.1, -127.7	9.2, -44.0	4.4, 36.9	1.2, 147.3	6, -41.5	.1, 71.3	5, -171.7
AB	12.8, -126.3	8.8, -43.7	4.3, 36.0	1.1, 141.9	.5, -35.3	.1, 81.4	4, -163.0
CH	12.1, -125.2	8.5, -42.8	4.0, 37.4	1.0, 149.1	5, -35.6	.1, 21.3	.4, 174.0
BU	11.1, -126.9	7.1, -41.3	3.2, 44.1	.8, 171.3	.5, -31.7	.1, 102.2	6, 19.3
PA	12.0, -126.6	7.9, -39.8	3.6, 43.5	.9, 160.6	.5, -28.2	.2, 64.3	4, -127.9
SS	11.9, -126.2	7.7, -38.7	3.5, 45.3	.9, 160.8	.5, -17.2	.1, 95.7	.3, -113.2
LR	11.0, -126.3	7.1, -39.5	3.0, 45.8	.8, 173.9	6, -29.2	.2, 19.8	.2, -119.2
DC	12.4, -126.1	7.8, -39.1	3.6, 45.7	.8, 162.3	.5, -7.8	.1, 139.9	.2, 158.1
LS	9.9, -127.4	6.4, -41.6	3.0, 44.0	.8, 156.8	.3, -12.4	.1, 55.8	.3, -136.3
TA	10.6, -130.3	6.7, -38.4	3.1, 55.6	.9, -160.7	7, -14.7	.1, 113.2	4, 179.7
BC	11.3, -126.3	7.6, -33.7	3.7, 54.2	.9, 169.0	.5, -8.2	.2, 71.8	.5, -163.2

although indications of irregular current flows were pointed out by Schmucker [1970]. Conductivity models of the fault at one location in central California indicate a conductivity ranging from 10^{-3} S/m on the west side of the fault, through 10^{-1} S/m within the fault zone, to 10^{-2} S/m on the east side of the fault [Mazzella and Morrison, 1976].

Direct evidence for the flow of tidally-induced currents in the fault zone is obtained from telluric data measured both parallel and perpendicular to the fault zone in central California. The amplitude spectrum obtained from telluric data between the sites along the fault near magnetometer station (HA) (Figure 1) shows a dominant M_2 peak (Figure 2). The relatively small S_3 and the absence of higher solar harmonics in the telluric data suggest that currents induced by Sq variations are relatively small. Furthermore, the relative S_1, S_2, and M_2 harmonic amplitudes have ratios similar to those of the ocean-tide spectra in this area.

Thus, it appears that the ocean tides, rather than Sq effects, are the dominant source of telluric currents along the fault. We attribute the tidal harmonics in the total-field spectrum to a combination of direct ocean tide induction effects [as seen by Larsen, 1968; Osgood et al., 1970; and Cochrane, 1974] and channeled currents in the fault zone.

Because of their deterministic behavior, the nonseismic noise due to these effects can easily be filtered from the magnetic data. Figure 3 shows unfiltered difference-field data and the residuals after removing harmonics S_1 through S_6 and M_2. The reduction in standard deviation by means of this technique is typically about 50%. We expect that the remaining noise is generated in part by nonharmonic ionospheric/magnetospheric disturbances. Such noise, which can be further reduced using transfer functions or Weiner filter techniques, will not be discussed further here.

Another interesting feature is evident in Table 1. This is the variation in harmonic amplitude with site location along the fault. A plot of harmonic amplitude against distance

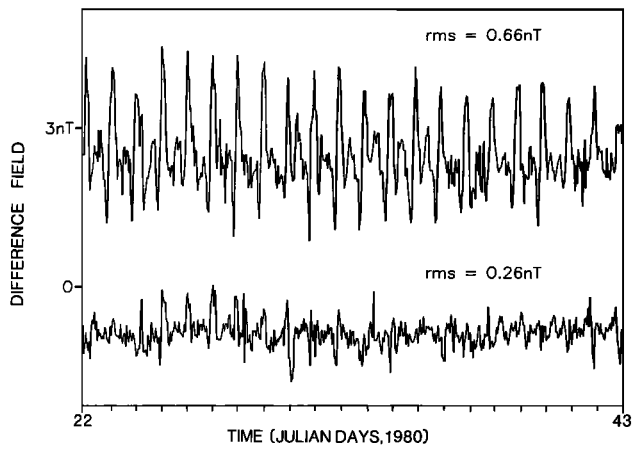

Fig. 3. Difference-field data from LE-HA and residual after filtering harmonics S_1 through S_6 and M_2.

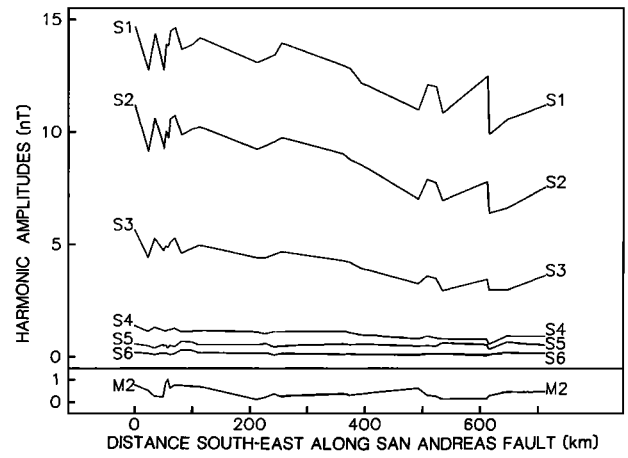

Fig. 4. Amplitudes of total-magnetic-field harmonics for 27 array sites in California.

along the fault (Figure 4) illustrates the general decreasing trend to the southeast for harmonics S_1 through S_3 which cannot be attributed to geographic variation of the Sq current system. Estimates of this geographic variation, from the northern to the southern limits of the array, spanning approximately 44° to 41° of geomagnetic latitude, were obtained by interpolating between the 5° Fourier amplitudes given by Campbell [1982]. These estimates are listed in Table 2, along with the observed variation taken from Table 1. While the 500 days of data (August, 1980 to January, 1982) used here to estimate Sq variation with latitude differs from that used by Campbell, checks of spectra during a quiet year (1975) agree with that in Figure 2. Nor can ocean induction effects account for this trend, since such effects are expected to decrease total field variations as the coast is approached - the opposite of the observed trend.

Alternatively, we argue that regional tectonic structure may be responsible for this behavior. Specifically, a hotter, more conductive crust and upper mantle under the array in southern California is suggested by elevated teleseismic velocities [Raikes and Hadley, 1979] and heat flow measurements in central and southern California [Lachenbruch and Sass, 1980]. The attenuation of solar harmonic amplitudes to the southeast can be attributed to increased induction in the associated conductive structures. Detailed study of comparative induction effects between central and southern California and across the fault system could quantify these effects.

Conclusions

The amplitude spectra of California geomagnetic data include M_2 tidal harmonics with amplitudes as large as 1 nT. We attribute this to a combination of ocean tide induction and inhomogeneous current channeling effects in the San Andreas fault zone. Thus, the presence of strong M_2 tidal harmonics in telluric-current data measured along the San Andreas fault provides independent evidence of current channeling in the fault. Straight forward

Table 2. Sq harmonic amplitude variation between 44° and 41° of geomagnetic latitude.

	S_1	S_2	S_3	S_4
calculated (nT)	0.07	1.31	0.16	-0.07
observed (nT)	2.7	3.1	0.91	0.45

harmonic filtering removes the tidal noise from these data. This allows a reduction of up to 60% in the standard deviation of the differenced magnetic field data. We find also that a regional trend of decreasing amplitudes for S_1, S_2, S_3 and S_4 to the southeast along the San Andreas fault cannot be accounted for by the geographical variation of Sq effects. Instead, we attribute this trend to induction in a hotter, thinner crust in southern California.

Acknowledgments. John Roger provided technical and logistic support for the telluric experiment. The IGPP Time Series Program, developed by Duncan Agnew was used extensively for data analysis. Support for R.H. Ware was provided by USGS Grant #14-08-0001-1940 and NSF Grant #EAR 79-20094.

References

Beahn, T.J., Geomagnetic field gradient measurements and noise reduction techniques in Colorado, J. Geophys. Res., 81, 6276-6280, 1976.

Campbell, W.H., Annual and semiannual changes of the quiet daily variations (Sq) in the geomagnetic field at North American locations, J. Geophys. Res., 87, 785-796, 1982.

Cochrane, N.A., Tidal influence on electric and magnetic fields recorded at coastal sites in Nova Scotia, Jour. Atm. Terr. Phys., 36, 49-54, 1974.

Davis, P.M., D.D. Jackson, C.A. Searls, and R.L. McPherron, Detection of tectonomagnetic events using multichannel predictive filtering. J. Geophys. Res., 86, 1731-1737, 1981.

Davis, P.M. and M.J.S. Johnston, Localized geomagnetic field changes near active faults in California, J. Geophys. Res. (in press), 1982.

Hewson-Browne, R.C., Magnetic effects of sea tides, Phys. Earth Planet. Interiors, 7, 161-185, 1973.

Johnston, M.J.S., B.E. Smith, and R. Mueller, Tectonomagnetic experiments and observations in western USA, J. Geomagn. Geoelec., 28, 85-97, 1976.

Johnston, M.J.S., Local magnetic variations and stress changes near a slip discontinuity on the San Andreas fault, J. Geomag. Geoelectr., 30, 511-522, 1978.

Lachenbruch, A.H. and J.H. Sass, Heat flow and energetics of the San Andreas fault zone, J. Geophys. Res., 85, 6185-6222, 1980.

Larsen, J.C., Electric and magnetic fields induced by deep sea tides, Geophys. J.R.A.S., 16, 47-70, 1968.

Malin, S.R.C., Ocean effects in geomagnetic tides, Annales de Geophysique, 33, 109-113, 1977.

Matsushita, S. and W.H. Campbell, Physics of geomagnetic phenomena, vol. 1, 302-424, Academic Press, N.Y., pp. 623, 1967.

Mazzella, A. and H.F. Morrison, Electrical resistivity variations associated with earthquakes on the San Andreas fault, Science, 185, 855-857, 1974.

Mueller, R.J., M.J.S. Johnston, B.E. Smith, and V. Keller, U.S. Geological Survey magnetometer network and measurement techniques in western USA, USGS Open File Report #81-1346, Menlo Park, CA, 1981.

Mueller, R.J. and M.J.S. Johnston, Precision of differential magnetometer measurements along the San Andreas fault, Trans A.G.U., 62, 1054, 1981.

Osgood, C., W.G.V. Rosser, and N.J.W. Webber, Electric and magnetic fields associated with sea tides in the English Channel, Phys. Earth Planet. Int., 4, 65-77, 1970.

Raikes, S.A. and D.M. Hadley, The azimuthal variation of teleseismic p-residuals in southern California: Implications for upper-mantle structure, Tectonophysics, 56, 89-98, 1979.

Schmucker, V., Anomalies of geomagnetic variations in the southwestern United States. Bull. Scripps. Inst. Oceanography, Vol. 13, 160 pp, 1970.

Stacey, F.D., The seismomagnetic effect, Pure Appl. Geophys., 58, 5-22, 1964.

Stacey, F.D. and S.K. Bannerjee, The physical principles of rock magnetism, Elsevier, 195 pp, 1974.

Ware, R.H., High-accuracy magnetic field difference measurements and improved noise reduction techniques for use in tectonomagnetic studies, J. Geophys. Res., 84, 6291-6296, 1979.

(Received September 3, 1982;
accepted October 19, 1982.)